

NACA RM L9L08


NACATECH LIBRARY KAFB, NM
0143805

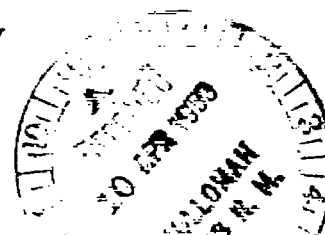

RESEARCH MEMORANDUM

AN INVESTIGATION OF A SUPERSONIC AIRCRAFT CONFIGURATION
HAVING A TAPERED WING WITH CIRCULAR-ARC
SECTIONS AND 40° SWEEPBACK

STATIC LONGITUDINAL STABILITY AND CONTROL
CHARACTERISTICS AT A MACH NUMBER OF 1.40

By M. Leroy Spearman


Langley Aeronautical Laboratory
Langley Air Force Base, Va.





**NATIONAL ADVISORY COMMITTEE
FOR AERONAUTICS**

WASHINGTON
April 3, 1950


19 05 12

Classification cancelled (or changed to UNCLASSIFIED)

By Authority of NASA Tech. Pub. Announcement #129
(OFFICER AUTHORIZED TO CHANGE)

By SP-5 JAL
NAME AND

SP-5 JAL
GRADE OF OFFICER MAKING CHANGE)

24 Mar 61
DATE



0143805

NACA RM L9L08

~~CONFIDENTIAL~~

NATIONAL ADVISORY COMMITTEE FOR AERONAUTICS

RESEARCH MEMORANDUM

AN INVESTIGATION OF A SUPERSONIC AIRCRAFT CONFIGURATION
HAVING A TAPERED WING WITH CIRCULAR-ARC
SECTIONS AND 40° SWEEPBACK

STATIC LONGITUDINAL STABILITY AND CONTROL
CHARACTERISTICS AT A MACH NUMBER OF 1.40

By M. Leroy Spearman

SUMMARY

An investigation has been conducted in the Langley 4- by 4-foot supersonic tunnel to determine the longitudinal stability and control characteristics of a model of a supersonic airplane configuration at a Mach number of 1.40. The model had a 40° sweptback wing with 10-percent-thick circular-arc sections normal to the quarter-chord line.

The results of the investigation indicated a high degree of longitudinal stability that was fairly constant throughout the trim-lift-coefficient range. The altitude and maneuverability in flight at a Mach number of 1.40 of an airplane similar to the model would be limited by the low maximum trim lift coefficient (0.38) attainable with the maximum negative stabilizer incidence available. The stabilizer hinge-moment parameters were large but, because of their linear nature, probably could be reduced by relocating the stabilizer pivot point.

INTRODUCTION

One of the important fields of research at supersonic speeds is that concerned with the problems of stability and control. A need exists for comprehensive wind-tunnel investigations of supersonic aircraft configurations to determine experimentally the stability and control characteristics at supersonic speeds. Such investigations should include the effects of various aircraft components on the

~~CONFIDENTIAL~~

50-542-6

over-all stability characteristics and provide experimental data for subsequent correlation with theoretical calculations. An investigation of two supersonic aircraft configurations has been made in the Langley 9-inch supersonic tunnel (reference 1); however, tests of only the complete models with fixed control surfaces were made.

An investigation has been conducted in the Langley 4- by 4-foot supersonic tunnel to determine the aerodynamic characteristics of a relatively large size model of one of the supersonic aircraft configurations utilized in reference 1. This model was equipped with a remotely controllable stabilizer, a movable rudder, and movable ailerons. In addition, the horizontal tail, vertical tail, wing, and canopies were detachable. Forces and moments acting on the model were measured by means of a six-component internal strain-gage balance and all control-surface hinge moments were measured by means of strain gages. Although complete longitudinal, lateral, and directional stability and control data as well as model-breakdown data have been obtained at Mach numbers of 1.40 and 1.59, this paper presents only the results of the longitudinal stability and control investigation at a Mach number of 1.40. A somewhat detailed description of the model, balance, and support system is included to serve as a reference for future papers.

COEFFICIENTS AND SYMBOLS

The results of the tests are presented as standard NACA coefficients of forces and moments and are referenced to the stability axes shown in figure 1. The reference center of gravity (indicated in fig. 2) is at the 25-percent mean aerodynamic chord.

The coefficients and symbols are defined as follows:

C_L	lift coefficient $\left(\frac{\text{Lift}}{qS} \right)$ where $\text{Lift} = -Z$
C_D	drag coefficient $\left(\frac{\text{Drag}}{qS} \right)$ where $\text{Drag} = -X$
C_m	pitching-moment coefficient $\left(\frac{M'}{qSc} \right)$
C_{H_t}	stabilizer hinge-moment coefficient $\left(\frac{H_t}{qS_t \bar{c}_t} \right)$
Z	force along Z-axis, pounds
X	force along X-axis, pounds

M'	pitching moment about Y-axis, foot-pounds
H_t	stabilizer hinge moment measured about 21-percent point of the stabilizer mean aerodynamic chord, foot-pounds
q	free-stream dynamic pressure, pounds per square foot
S	wing area, square feet
S_t	stabilizer area, square feet
\bar{c}	wing mean aerodynamic chord, feet $\left(\frac{2}{S} \int_0^{b/2} c^2 dy \right)$
c	airfoil section chord, feet
y	distance along wing span, feet
\bar{c}_t	stabilizer mean aerodynamic chord, feet
α	angle of attack of fuselage center line, degrees
i_t	stabilizer incidence angle with respect to fuselage center line, degrees
ϵ	effective downwash angle, degrees
C_{m_t}	increment of pitching-moment coefficient provided by the tail
L/D	ratio of lift to drag (C_L/C_D)
W/S	wing loading, pounds per square foot
$\partial C_m / \partial i_t$	stabilizer effectiveness, rate of change of pitching-moment coefficient with stabilizer incidence angle
$\partial \epsilon / \partial \alpha$	rate of change of downwash angle with angle of attack
C_{L_α}	trim-lift-curve slope
$\partial C_m / \partial C_L$	rate of change of pitching-moment coefficient with lift coefficient
M	Mach number

$C_{h\alpha}$ rate of change of stabilizer hinge-moment coefficient
with angle of attack $\left(\left(\frac{\partial C_{ht}}{\partial \alpha} \right)_{i_t} \right)$

C_{hs} rate of change of stabilizer hinge-moment coefficient
with stabilizer incidence angle $\left(\left(\frac{\partial C_{ht}}{\partial i_t} \right)_{\alpha} \right)$

APPARATUS

Tunnel

The Langley 4- by 4-foot supersonic tunnel in which the tests were conducted is a closed-throat single-return tunnel having a nominal Mach number range of 1.2 to 2.2. Changes in Mach number are effected through the use of a flexible wall nozzle. With the present drive motor of 6000 horsepower, the operating stagnation pressure of the tunnel is limited to a maximum of 0.3 atmosphere.

Model and Support System

A three-view drawing of the model is shown in figure 2 and the geometric characteristics are presented in table I. The model selected for these tests had a wing with 40° of sweep at the quarter-chord line, aspect ratio 4, taper ratio of 0.5, and was composed of symmetrical 10-percent-thick circular-arc sections in a plane normal to the quarter-chord line. For the basic stability investigation, the wing was equipped with flat-sided ailerons with a blunt trailing edge having a thickness 0.5 of the hinge-line thickness. The fuselage and canopy coordinates are given in reference 2.

The aileron and rudder were adjustable and were set manually. The angle of incidence of the stabilizer was remotely controlled through the use of an electric motor housed within the fuselage. The horizontal tail, vertical tail, canopies, and wing were detachable in order to facilitate the testing of various combinations (fig. 3).

The model was mounted on a sting support that provides angular movements in a horizontal plane in such a manner that the model remains approximately in the center of the test section. Details of the support system are shown in figure 4. The model and support at a negative angle of attack are shown in figure 5. An angle of $\pm 11^\circ$ may be obtained before the rear of the sting touches the tunnel side wall. By traversing the

sting laterally so that the model moves about 10 inches from the vertical center line of the tunnel, the angle range may be extended to $\pm 16.3^\circ$. The angular range can be extended further through the use of bent stings. Stings having fixed bends of 3° and 6° at a point about 1 inch to the rear of the model base have been used. The model and stings could be rotated so that tests could be made in the angle-of-attack plane at fixed yaw angles (wing vertical) or in the angle-of-yaw plane at fixed angles of attack (wing horizontal).

Balance

The model was equipped with a special six-component wire-strain-gage internal balance. The balance was temperature compensated and the interaction between components was within the accuracy of the scale readings. Forces and moments on the balance were transmitted to a Brown self-balancing potentiometer from which individual readings of the six components were visually recorded. A selector switch for each component provided four scale ranges so that the sensitivity of the system could be increased for conditions of low loading.

Hinge moments for the rudder, aileron, and stabilizer were obtained through the use of wire-strain-gage balances with separate dial indicators provided for each control surface.

The six-component balance and the hinge-moment balances were calibrated in the laboratory and in place in the tunnel and were checked before and after and frequently during the test program.

TESTS

Test Conditions

All tests were conducted at a Mach number of 1.40 with a stagnation pressure of $1/4$ atmosphere and a stagnation temperature of 110° F. The calibration of the Mach number 1.40 nozzle is presented in reference 3. The stagnation dew point was maintained at -25° F or less so that adverse condensation effects might be prevented (reference 3).

The dynamic pressure for the tests was about 229 pounds per square foot and the Reynolds number based on a mean geometric chord of 0.557 foot was about 6×10^5 .

Corrections and Accuracy

No attempt was made to evaluate the tare forces caused by sting interference and no tares were applied to the results. Though it is indicated that the tare forces caused by sting interference are small (reference 4), the exact magnitude is not known.

Sting deflection under load was negligible and no angle-of-attack correction was necessary. The variation in Mach number in the vicinity of the model due to flow irregularities is about ± 0.01 . The flow angularity in the horizontal plane is about $\pm 0.2^\circ$ and in the vertical plane about 0.27° to -0.11° . Tests made with the model in the horizontal plane at 6° angle of attack (using 6° bent sting) indicated excellent agreement with data obtained with the model in the vertical plane at 6° angle of attack using the straight sting. These data are included in the figures as an indication of the small effect of the bent sting and of the flow angularity on the test results.

The maximum uncertainties in the aerodynamic coefficients (due to the balance system) are as follows:

Normal force	± 0.0011
Chord force	± 0.00034
Pitching moment	± 0.00045
Stabilizer hinge moment	± 0.0013
Lift	± 0.0010
Drag	± 0.00025

These uncertainties in the coefficients are maximum instrument variations due to zero shift and sensitivity of the system and have been combined into a precision measure by the method of reference 5. Although normal and chord forces were directly recorded by the balance system, in the calculation of the data these components were combined to obtain lift and drag. Repeated calibrations of the balance showed small changes in slope (0.75 percent or less) over relatively long periods of time. The effects of these changes have been neglected because the results presented in this paper were obtained immediately following the initial calibration. Since the interactions between components were small they were also neglected.

The angle of attack was accurate to $\pm 0.05^\circ$, the tail incidence angle was accurate to $\pm 0.1^\circ$, and the dynamic pressure could be determined within 0.25 percent.

Base pressure measurements were not obtained for the Mach number 1.40 tests but were obtained for the Mach number 1.59 tests. These data indicate that if the drag is based on free-stream static pressure the drag correction would be within the accuracy of the scale readings except

for the angle-of-attack range from 4° to 10° where the correction would result in drag about 1 percent less than that presented.

Test Procedure

The longitudinal tests covered an angle-of-attack range from -4° to 10° with a range of stabilizer angles from 3.7° to -10.2° . The stabilizer angles were selected to maintain conditions near trim. In addition, one test was made with the stabilizer removed.

DISCUSSION

The variation with lift coefficient of the angle of attack, pitching-moment coefficient, and drag coefficient for several stabilizer deflections is presented in figure 6. (Included in the figure is a check point for each component obtained with the model in a horizontal position in order to illustrate the concordance with results obtained with the model in the vertical position.)

An attempt has been made to show the manner in which the various longitudinal-stability determinants influence the total stability of the model. Assuming that the tail does not affect the lift-curve slope of the complete model and that the stabilizer effectiveness is independent of angle of attack, the static longitudinal stability may be expressed as

$$\frac{\partial C_m}{\partial C_L} = \left(\frac{\partial C_m}{\partial C_L} \right)_0 + \frac{\partial C_m}{\partial i_t} \left(1 - \frac{\partial \epsilon}{\partial \alpha} \right) \frac{1}{C_{L_\alpha}}$$

where $\left(\frac{\partial C_m}{\partial C_L} \right)_0$ is the static longitudinal stability with the tail off

and $\frac{\partial C_m}{\partial i_t} \left(1 - \frac{\partial \epsilon}{\partial \alpha} \right) \frac{1}{C_{L_\alpha}}$ is the contribution of the tail to the total static longitudinal stability. The variation of the effective downwash angle with angle of attack determined from the relation $\epsilon = \alpha + i_t - \frac{C_{m_t}}{\partial C_m / \partial i_t}$

is presented in figure 7. A summary plot of the static-longitudinal-stability determinants as obtained from the data of figure 6 is shown in figure 8. From the data of figure 8 and the expression for the static longitudinal stability, the relative effects of the various determinants

on the total stability can be obtained. In general, the complete model exhibits a large degree of static longitudinal stability that remains fairly constant through the trim-lift-coefficient range. In the lift-coefficient range up to $C_L = 0.16$ a rearward shift of the wing-fuselage aerodynamic center is apparently counteracted by an increase in $C_{L\alpha}$ and $\partial\epsilon/\partial\alpha$ so that no change in the complete-model stability occurs. The slight changes in stability indicated in the C_L range from 0.16 to 0.38 are largely a function of the wing-fuselage aerodynamic-center shift inasmuch as the decreasing $C_{L\alpha}$ and increasing $\partial\epsilon/\partial\alpha$ tend to compensate each other. The stabilizer effectiveness $\partial C_m/\partial i_t$ remains unchanged through the trim-lift range and hence provides a constant contribution to the total stability.

The high degree of stability that exists for the configuration tested could be reduced by shifting the center of gravity rearward; however, the center-of-gravity location is a result of low-speed stability considerations (reference 6) and to decrease the stability at a Mach number of 1.40 in this manner while maintaining the same low-speed stability would entail a variable center-of-gravity location.

Because of the low value of maximum trim lift coefficient attainable with the maximum negative stabilizer incidence available, the altitude and maneuverability for a given wing loading of a full-scale airplane similar to the model would be limited. The variation with wing loading of the lift coefficient required for level flight at various altitudes is shown in figure 9. For a wing loading of 50 the maximum normal acceleration at 40,000 feet is about 4.1g and at 60,000 feet about 1.5g.

The variation of stabilizer hinge-moment coefficient with lift coefficient for various stabilizer angles is presented in figure 10 and the variation of stabilizer hinge-moment coefficient with stabilizer incidence for various angles of attack is presented in figure 11. The hinge-moment parameters $C_{h\alpha}$ and $C_{h\delta}$ both have values of about -0.01. Fairly large values of hinge moments are indicated. For an airplane flying at 60,000 feet, for example, the stabilizer hinge moment at the highest trim lift coefficient would be about 70 foot-pounds per square foot of stabilizer area. The hinge-moment parameters are linear, however, and their value probably could be reduced through a rearward movement of the stabilizer pivot point.

The lift-drag ratio for trimmed conditions is presented in figure 12. A maximum value of about 3.2 was obtained at the highest trim lift coefficient.

CONCLUDING REMARKS

The results of the static longitudinal stability and control investigation conducted at a Mach number of 1.40 on a model of a supersonic aircraft configuration having a 40° sweptback wing indicated a high degree of longitudinal stability that was fairly constant through the trim-lift-coefficient range.

The maximum trim lift coefficient attainable with the maximum negative stabilizer incidence available was low so that for an airplane similar to the model the altitude and maneuverability in flight would be limited. The stabilizer hinge-moment parameters were large but, because of their linear nature, probably could be reduced by relocating the stabilizer pivot point.

A maximum lift-drag ratio of about 3.2 was obtained at the highest trim lift coefficient.

Langley Aeronautical Laboratory
National Advisory Committee for Aeronautics
Langley Air Force Base, Va.

REFERENCES

1. Ellis, Macon C., Jr., Hasel, Lowell E., and Grigsby, Carl E.:
Supersonic-Tunnel Tests of Two Supersonic Airplane Model
Configurations. NACA RM L7J15, 1947.
2. Cooper, Morton, Smith, Norman F., and Kainer, Julian H.: A Pressure-
Distribution Investigation of a Supersonic Aircraft Fuselage and
Calibration of the Mach Number 1.59 Nozzle of the Langley 4- by
4-Foot Supersonic Tunnel. NACA RM L9E27a, 1949.
3. Hasel, Lowell E., and Sinclair, Archibald R.: A Pressure-Distribution
Investigation of a Supersonic-Aircraft Fuselage and Calibration of
the Mach Number 1.40 Nozzle of the Langley 4- by 4-Foot Supersonic
Tunnel. NACA RM L50B14a, 1950.
4. Osborne, Robert S.: High-Speed Wind-Tunnel Investigation of the
Longitudinal Stability and Control Characteristics of a $\frac{1}{16}$ -Scale
Model of the D-558-2 Research Airplane at High Subsonic Mach
Numbers and at a Mach Number of 1.2. NACA RM L9C04, 1949.
5. Michels, Walter C.: Advanced Electrical Measurements. Second ed.,
D. Van Nostrand Co., Inc., 1941.
6. Weil, Joseph, Comisarow, Paul, and Goodson, Kenneth W.: Longitudinal
Stability and Control Characteristics of an Airplane Model Having
a 42.8° Sweptback Circular-Arc Wing with Aspect Ratio 4.00,
Taper Ratio 0.50, and Sweptback Tail Surfaces. NACA RM L7G28, 1947.

TABLE I.- GEOMETRIC CHARACTERISTICS OF MODEL

Wing:

Area, sq ft	1.158
Aspect ratio	4
Sweepback of quarter-chord line, deg	40
Taper ratio	0.5
Mean aerodynamic chord	0.557
Airfoil section normal to quarter-chord line	10 percent thick, circular arc
Twist, deg	0

Horizontal tail:

Area, sq ft	0.196
Aspect ratio	3.72
Sweepback of quarter-chord line, deg	40
Taper ratio	0.5
Airfoil section	NACA 65-008

Vertical tail:

Area (exposed), sq ft	0.172
Aspect ratio (based on exposed area and span)	1.17
Sweepback of leading edge, deg	40.6
Taper ratio	0.337
Airfoil section, root	NACA 27-010
Airfoil section, tip	NACA 27-008

Fuselage:

Fineness ratio (neglecting canopies)	9.4
--	-----

Miscellaneous:

Tail length from $\bar{c}/4$ wing to $\bar{c}_t/4$ tail, ft	0.917
Tail height, wing semispans above fuselage center line	0.153



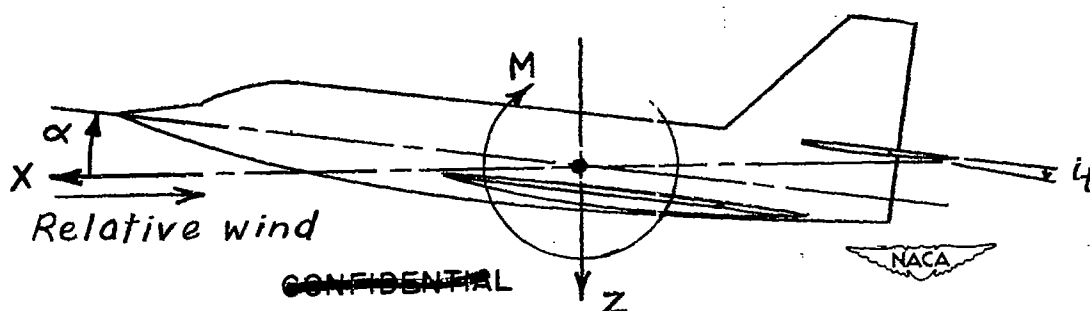
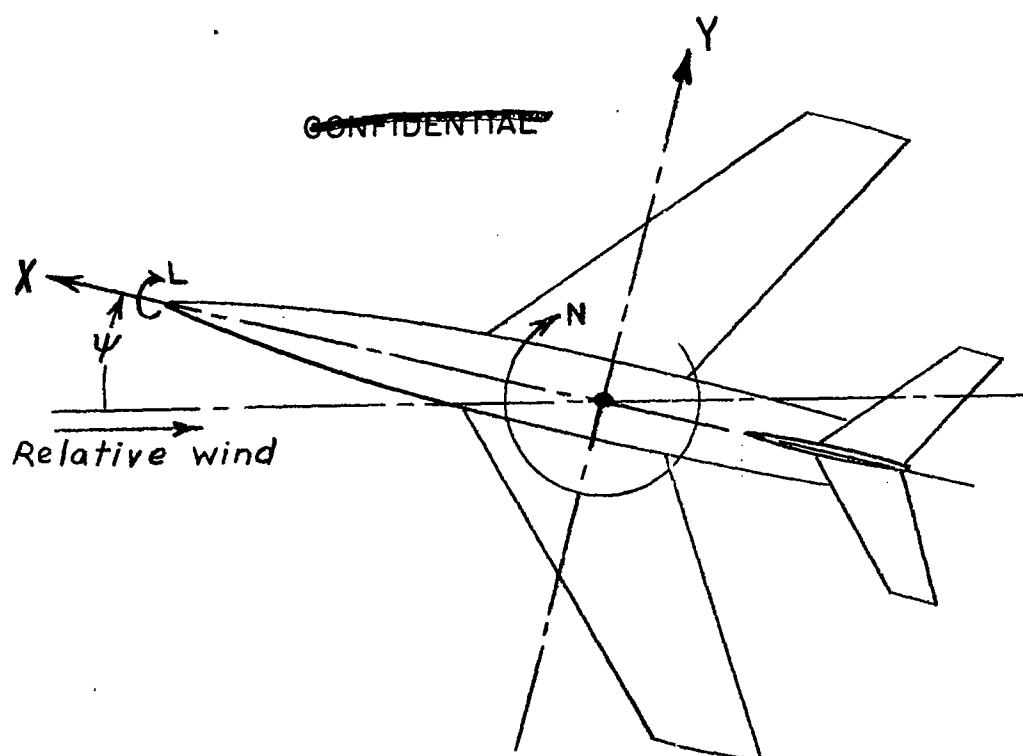


Figure 1.- System of stability axes. Arrows indicate positive values.

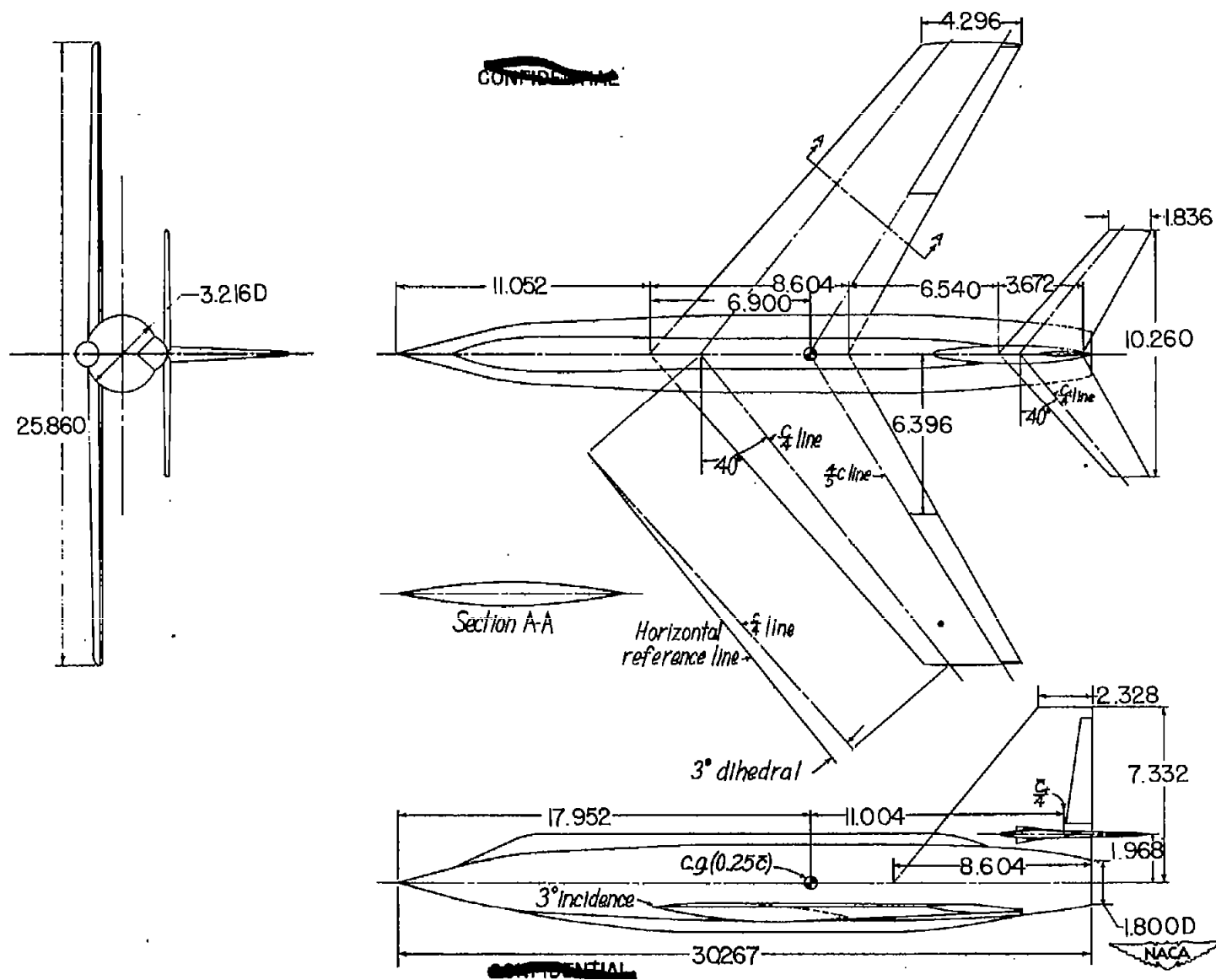
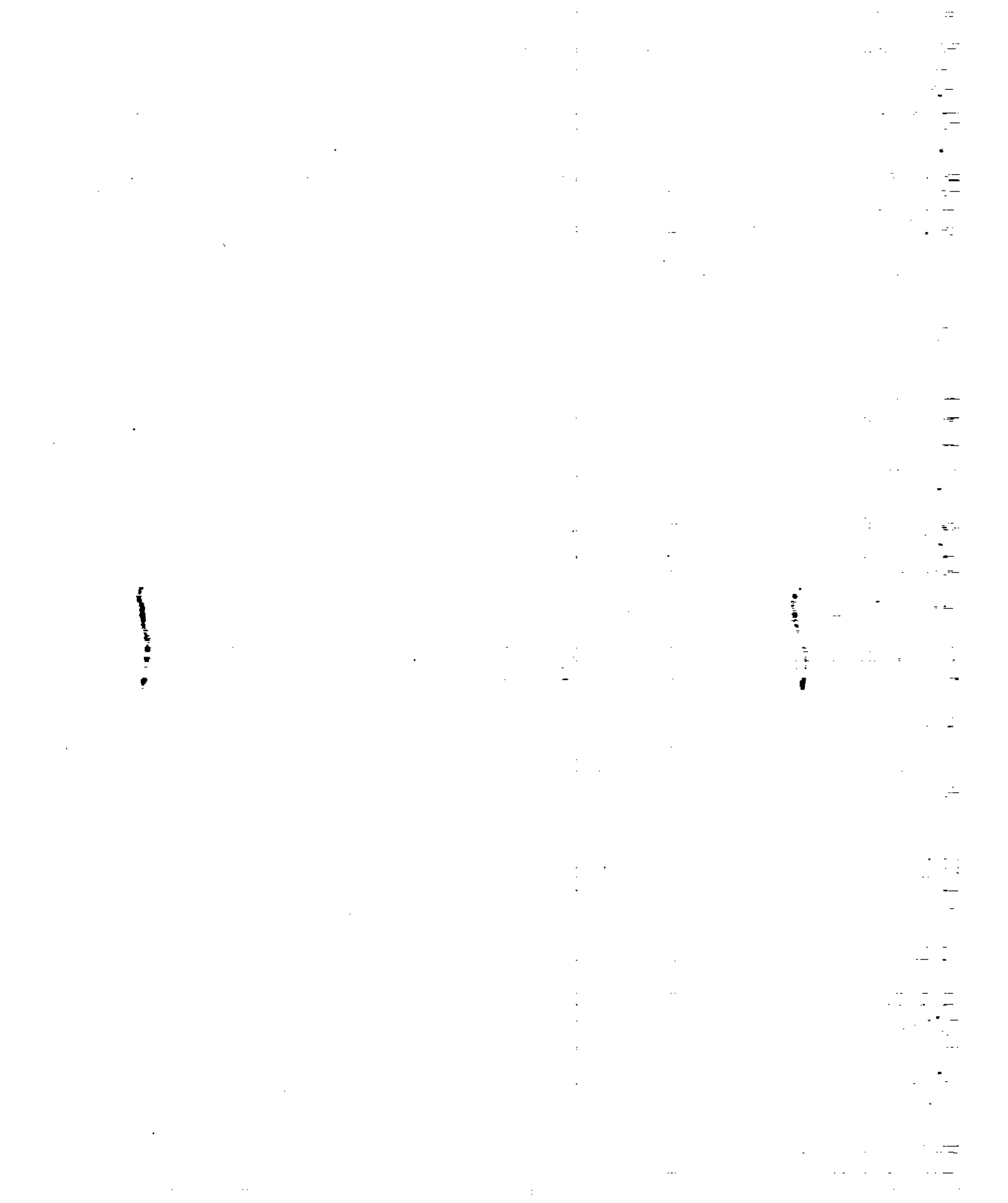


Figure 2.- Details of model of supersonic aircraft configuration. Dimensions in inches unless otherwise noted.



~~CONFIDENTIAL~~

NACA RM L9108

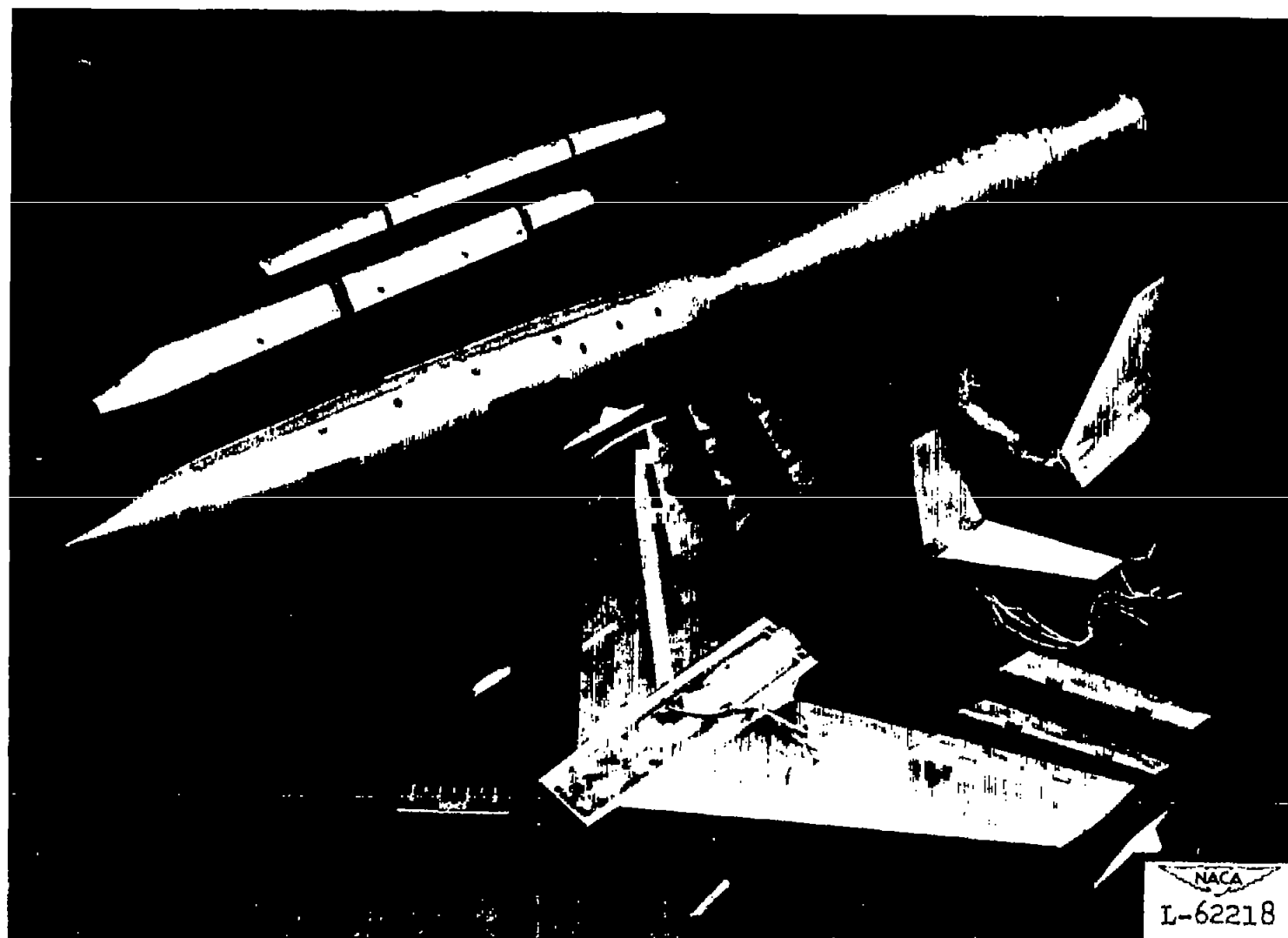


Figure 3.- Component parts of model of supersonic aircraft.

~~CONFIDENTIAL~~

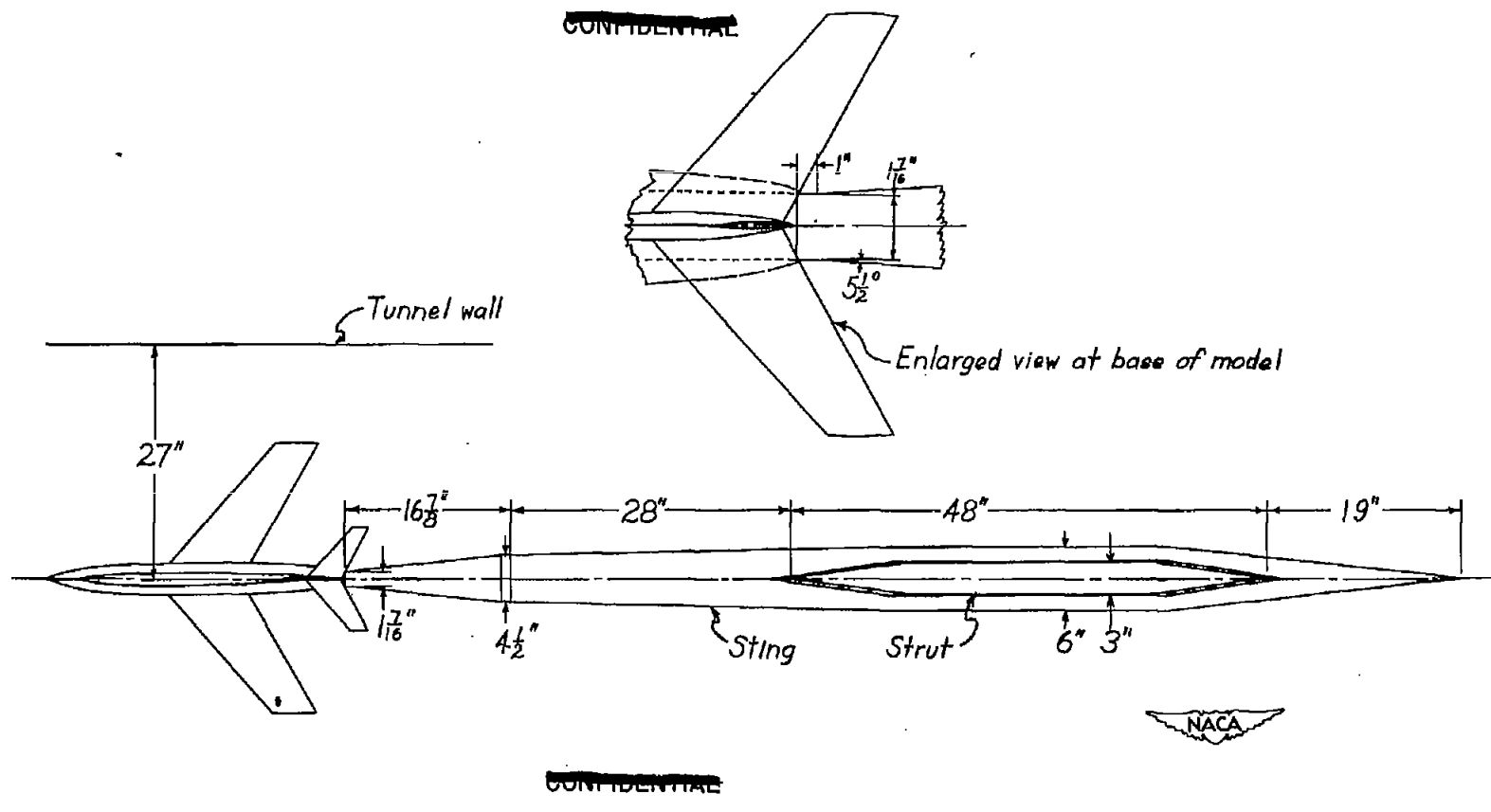
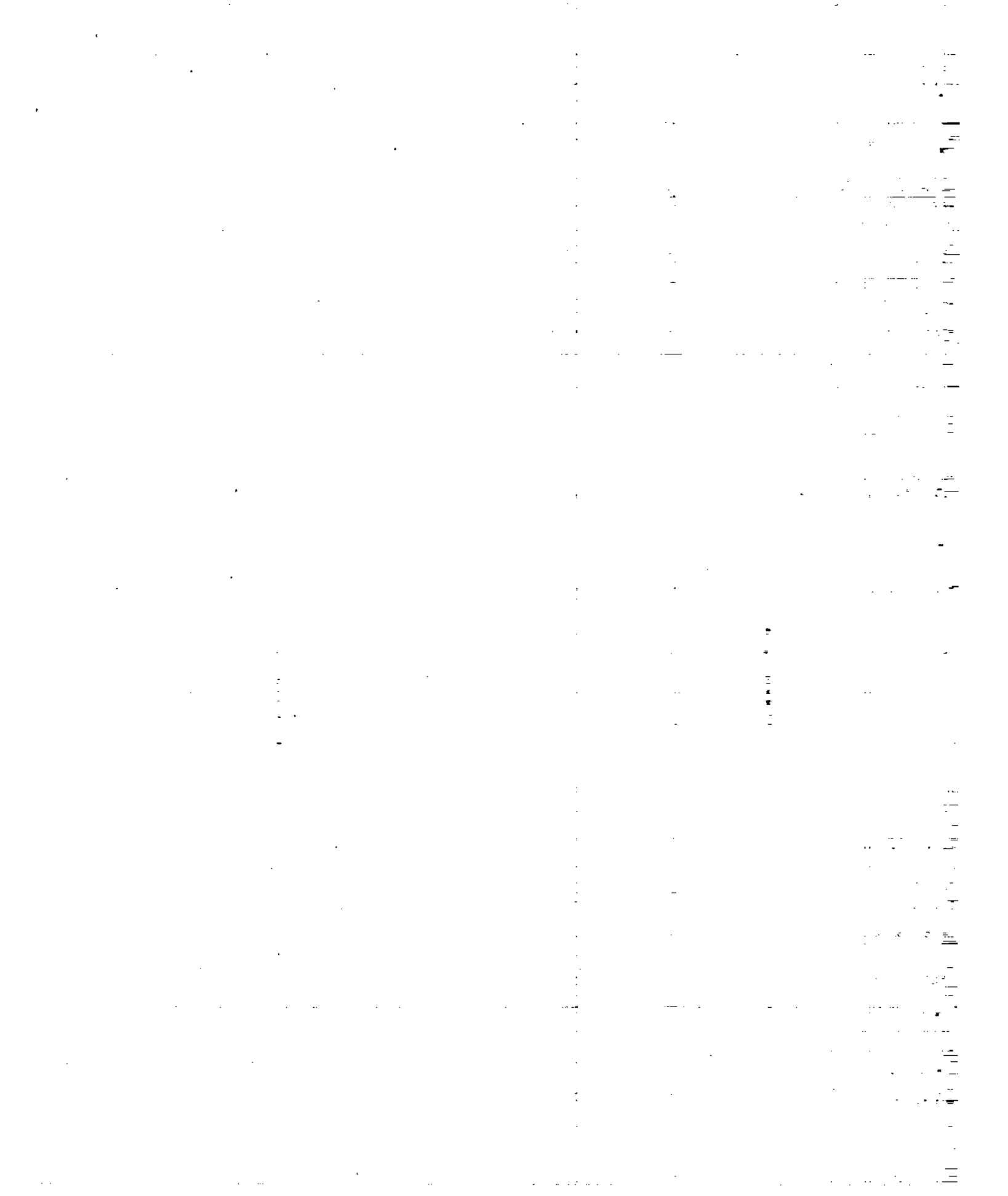


Figure 4.- Details of model support system.



~~CONFIDENTIAL~~

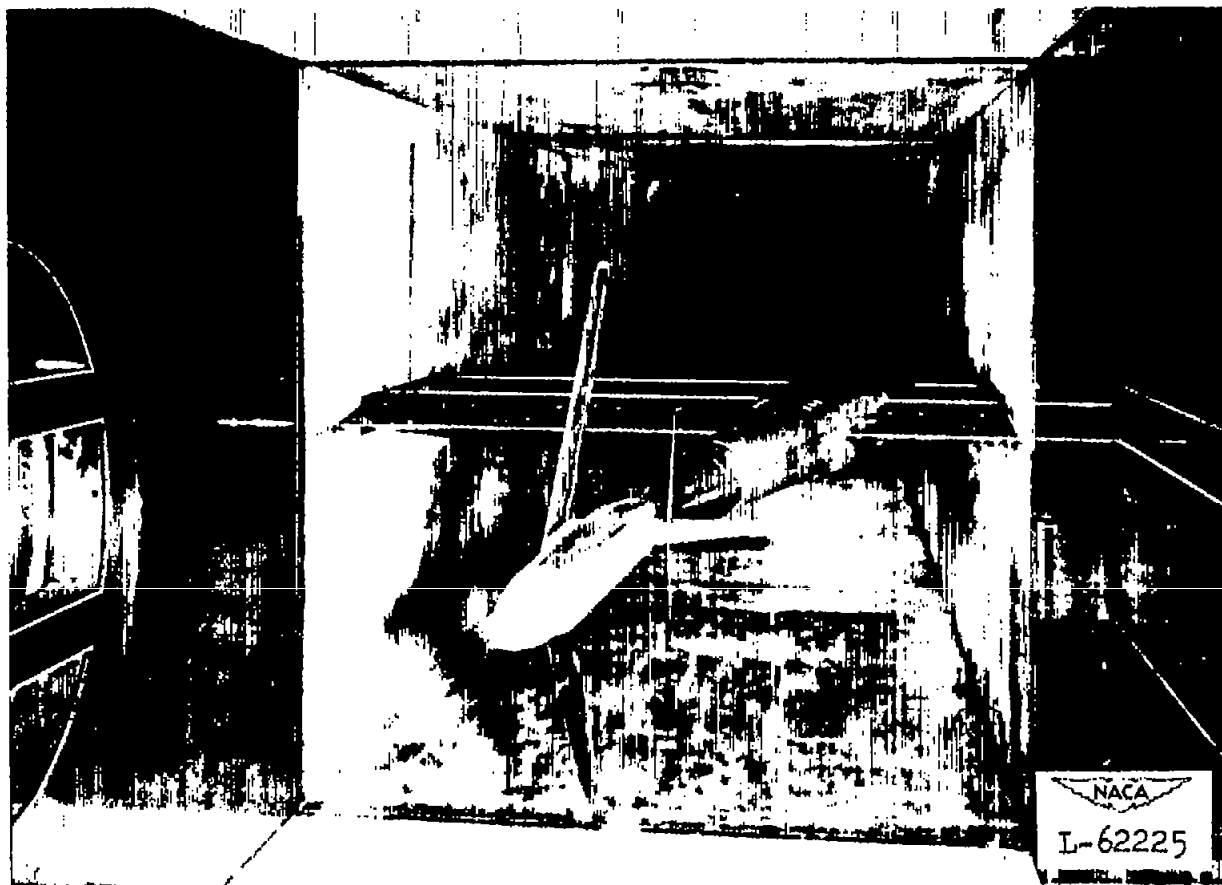


Figure 5.- Model of supersonic aircraft mounted in the Langley 4- by 4-foot supersonic tunnel.

~~CONFIDENTIAL~~

● 中国书画函授大学肇庆分校

100

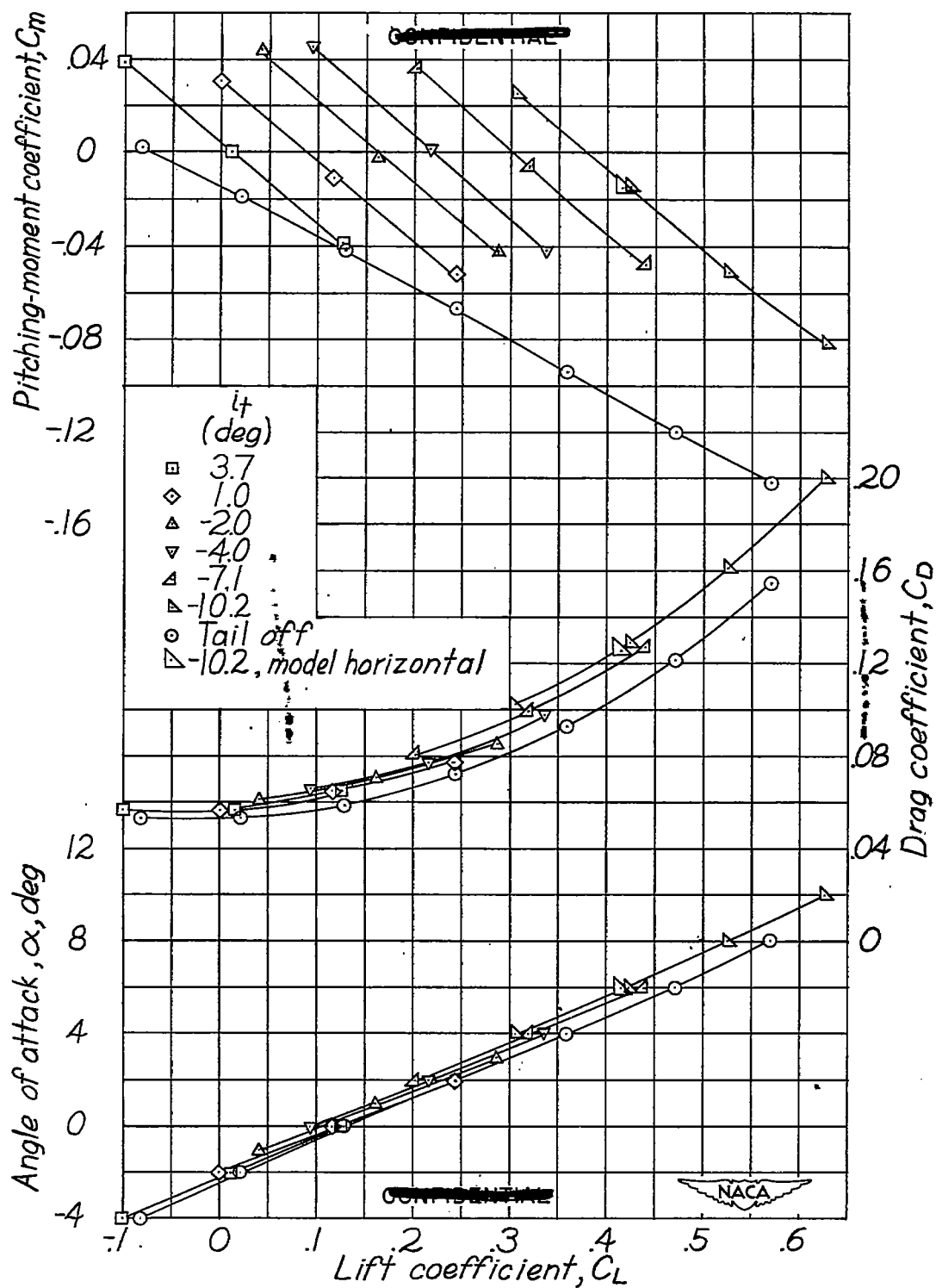


Figure 6.- Effect of stabilizer deflection on the aerodynamic characteristics in pitch. $M = 1.40$.

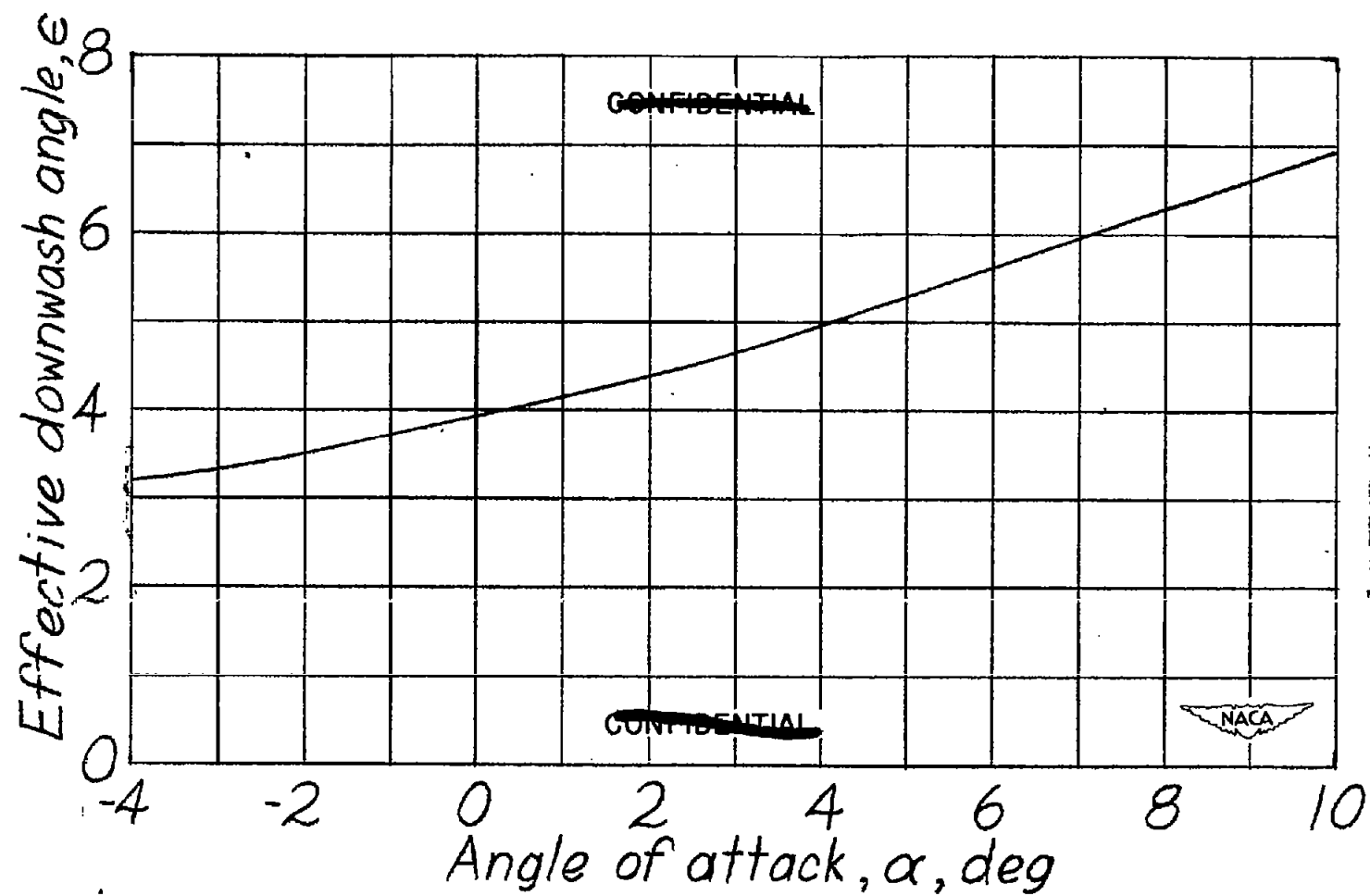


Figure 7.- Variation of effective downwash angle with angle of attack. $M = 1.40$.

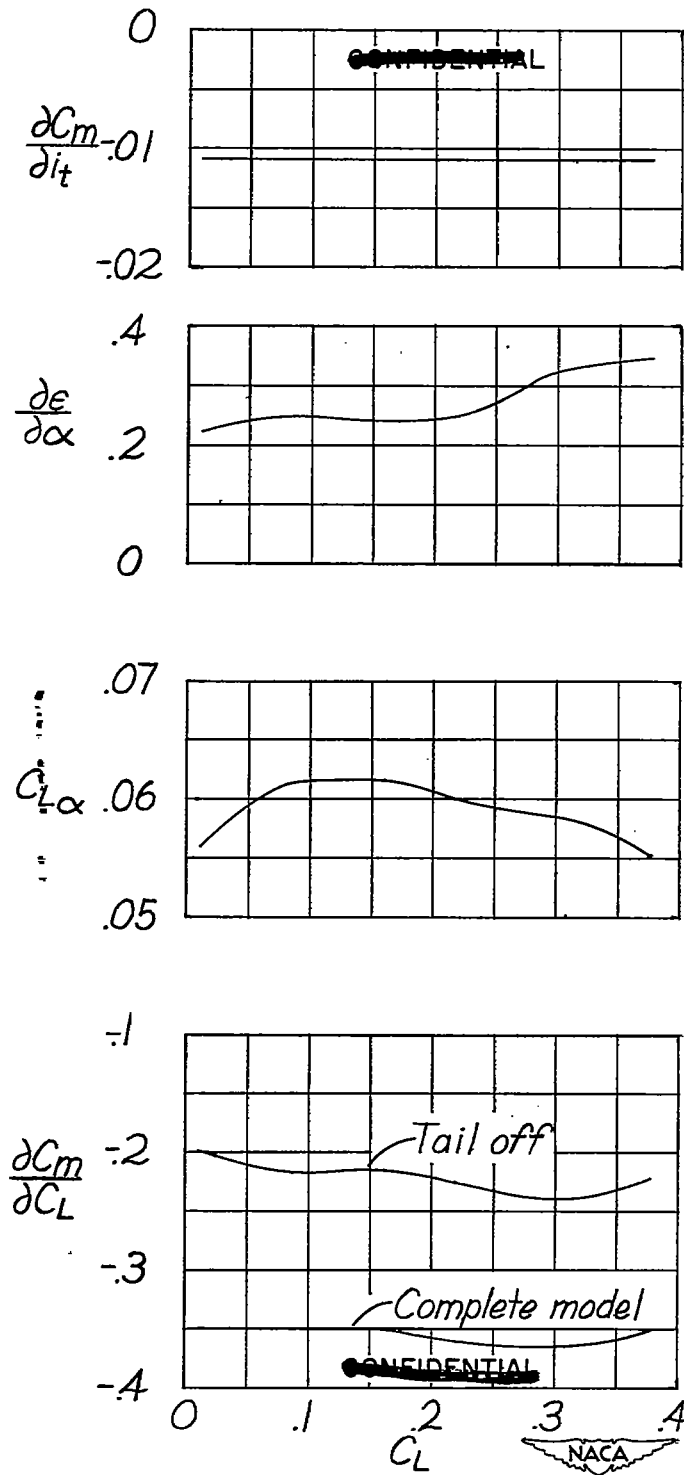


Figure 8.- Variation of the static-longitudinal-stability determinants with lift coefficient. $M = 1.40$.

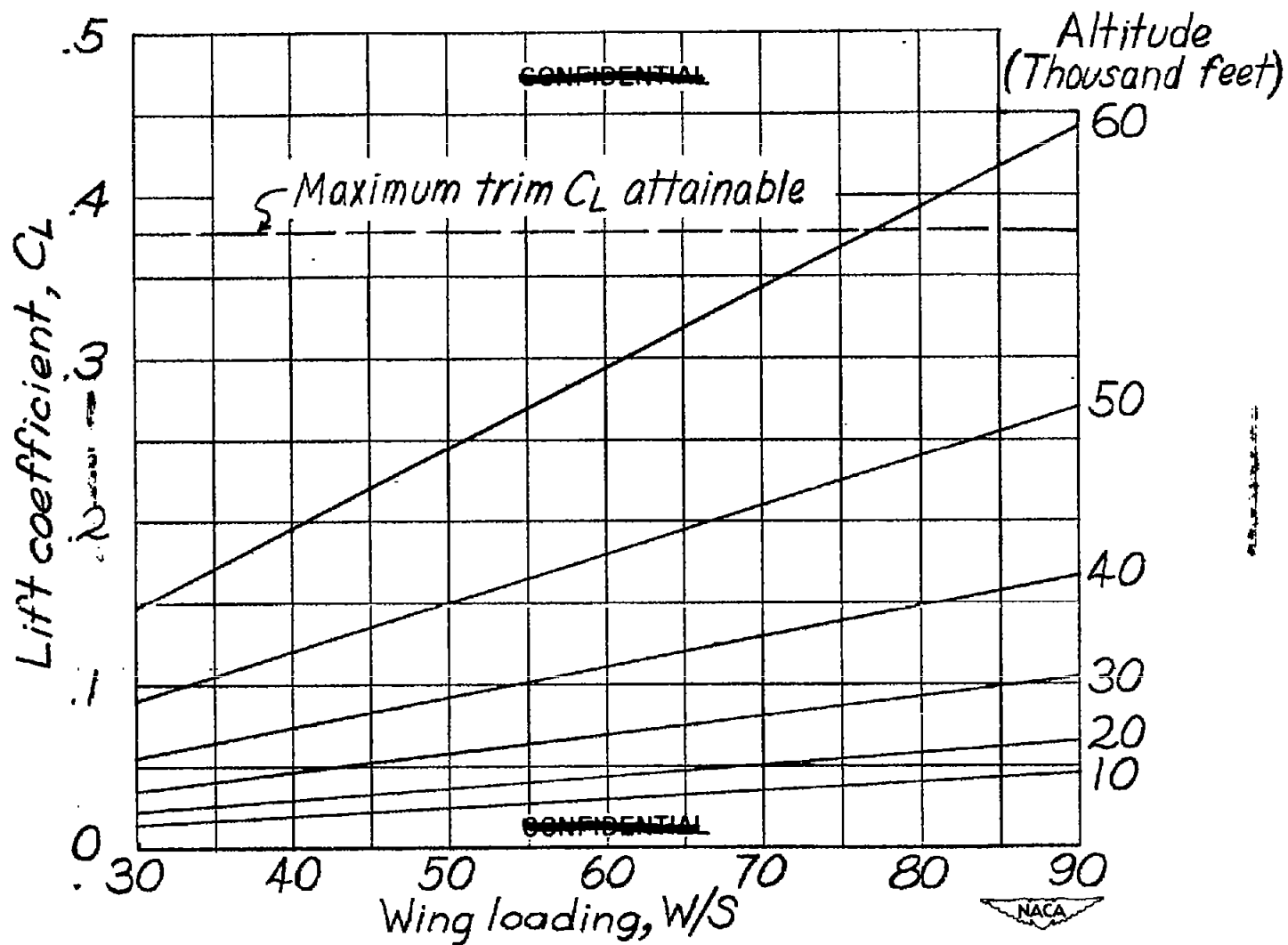


Figure 9.- Variation with wing loading of the lift coefficient for trim. $M = 1.40$.

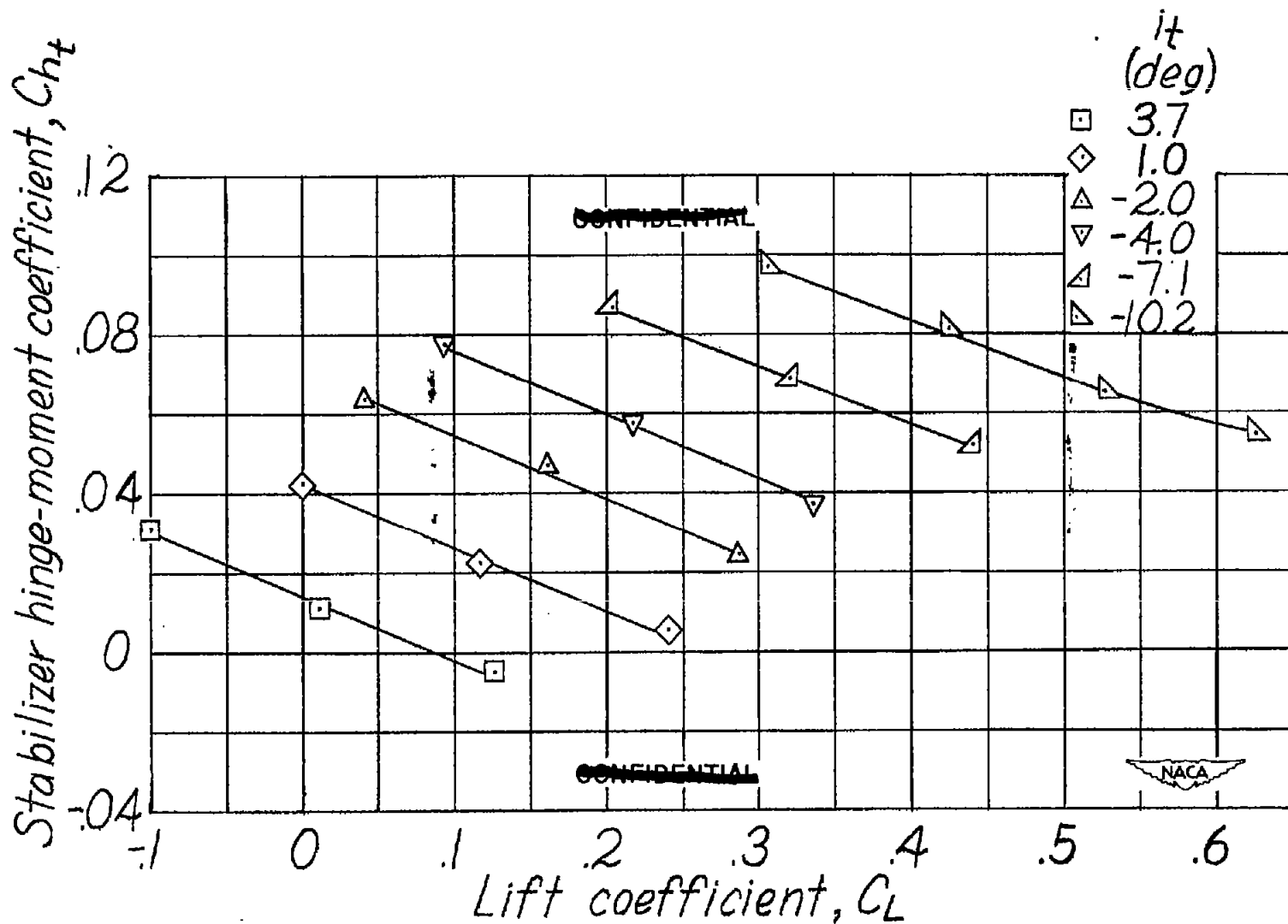


Figure 10.- Effect of stabilizer deflection on the stabilizer hinge-moment coefficient. $M = 1.40$.

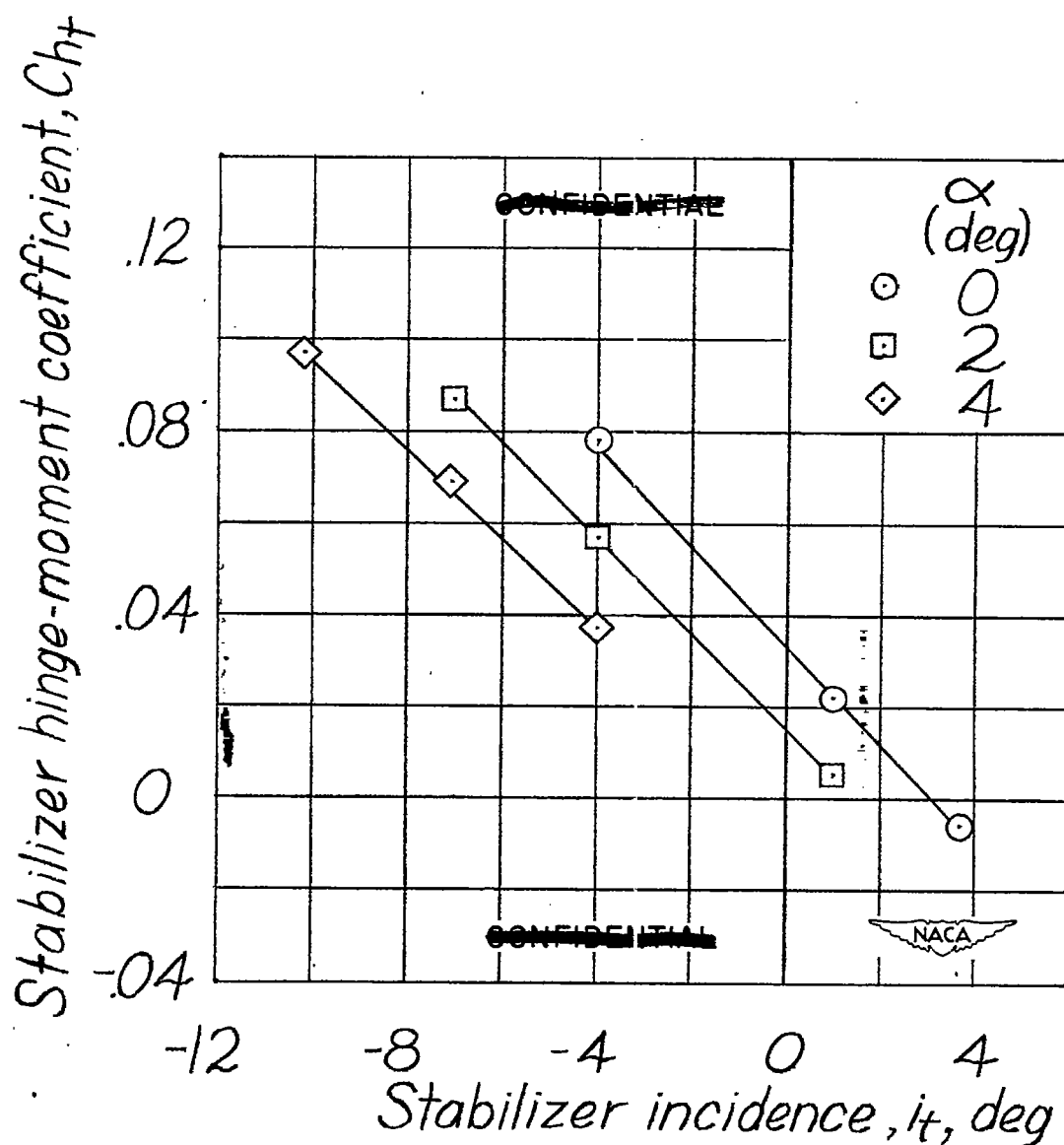


Figure 11.- Variation of stabilizer hinge-moment coefficient with stabilizer incidence. $M = 1.40$.

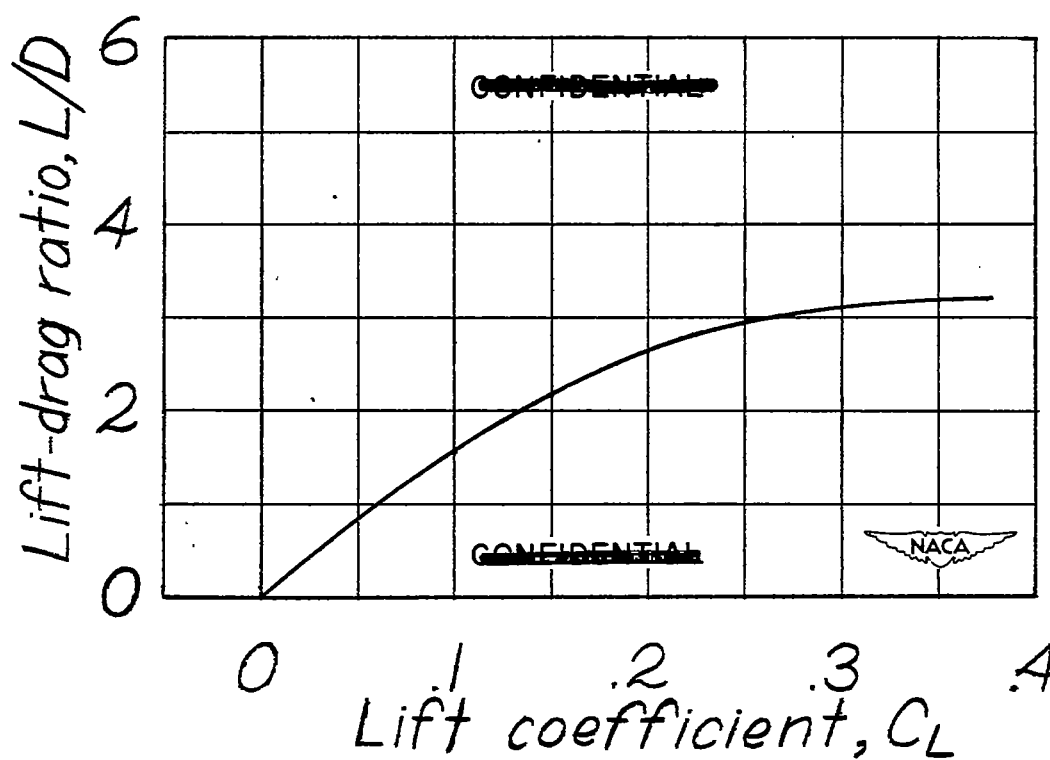


Figure 12.- Variation of lift-drag ratio with lift coefficient. $M = 1.40$.